nature immunology

Defining B cell immunodominance to viruses

Davide Angeletti[1], James S Gibbs[1], Matthew Angel[1], Ivan Kosik[1], Heather D Hickman[1], Gregory M Frank[1], Suman R Das[1,2], Adam K Wheatley[3], Madhu Prabhakaran[3], David J Leggat[3], Adrian B McDermott[3] & Jonathan W Yewdell[1]

Immunodominance (ID) defines the hierarchical immune response to competing antigens in complex immunogens. Little is known regarding B cell and antibody ID despite its importance in immunity to viruses and other pathogens. We show that B cells and serum antibodies from inbred mice demonstrate a reproducible ID hierarchy to the five major antigenic sites in the influenza A virus hemagglutinin globular domain. The hierarchy changed as the immune response progressed, and it was dependent on antigen formulation and delivery. Passive antibody transfer and sequential infection experiments demonstrated 'original antigenic suppression', a phenomenon in which antibodies suppress memory responses to the priming antigenic site. Our study provides a template for attaining deeper understanding of antibody ID to viruses and other complex immunogens.

Immunodominance is the phenomenon of unequal immunogenicity between different immunogens and different epitopes on the same immunogen. Although there is reasonably good understanding of $CD8^+$ T cell ID[1], far less is known about B cell and antibody (Ab) ID. Indeed, the promise of 'universal vaccines' for antigenically variable viruses, such as HIV and influenza A virus (IAV), based on targeting conserved regions of viral proteins[2,3] in large part depends on circumventing the immune system's marked tendency to focus on variable epitopes[4,5].

IAV is a relatively complex antigen. Virions contain at least ten viral gene products[6], and infected cells express at least five additional gene products that are potentially immunogenic in virus-infected hosts. Of these, hemagglutinin (HA) is of prime importance for vaccines. Only Abs specific for HA efficiently prevent infection, which is achieved by blocking HA-mediated attachment to the cell surface or HA-mediated fusion of viral and host cell membranes[7]. Although other viral proteins are more abundant in virions, HA is immunodominant in serum Ab responses to virions in mammals, birds and, remarkably, even lamprey despite the enormous structural difference between the Abs of jawed vertebrates and lamprey[8]. Intense interest in HA immunogenicity is based on the importance of antigenic drift in HA, necessitating annual re-vaccination with ever-updated IAV strains.

Classical studies with monoclonal Ab (mAb) escape mutants defined five non-overlapping antigenic sites in the globular domain of HA from the PR8 (H1) strain of IAV as the major target of virus-neutralizing Abs[9–11]. The Sa and Sb sites are located on the tip of the globular head of the homotrimeric molecule, whereas the Ca1, Ca2 and Cb sites are located toward the stem structure that supports the head and attaches the HA to the virion. Pioneering studies examined the anti-HA ID hierarchy by using anti-HA B cell hybridomas that were generated from IAV-immunized BALB/c mice. These revealed the early predominance of Cb-specific hybridomas, followed by a prevalence of Sb-specific hybridomas after secondary immunization[12–14]. Because the work was limited to hybridomas, it remains uncertain how representative the findings are for B cells and serum Abs. Here we generated a panel of Ab-selected IAV escape mutants. This tool allowed us to dissect B cell and polyclonal Ab ID at the level of individual antigenic sites.

RESULTS

Δ4 viruses preserve one intact antigenic site

The PR8 HA has five non-overlapping antigenic sites on its globular head that are targets of the large majority of the Ab response (**Fig. 1a**)[8–10,15]. To investigate immunodominance in B cell responses we generated a panel of viruses with multiple mutations that would enable facile determination of B cell and serum Ab specificity. The goal was to produce five 'Δ4' viruses—viruses in which one antigenic site was identical to the parental virus, whereas the other four sites were antigenically altered.

We initially used panels of selecting mAbs to determine the minimal number of mutations that would be required to abrogate the antigenicity of each antigenic site. Using this information, we attempted but ultimately failed to directly genetically engineer the ideal panel of viruses to maintain a consistent sequence at each of the mutated sites in the Δ4 viruses in the panel. This failure echoed our previous observations in generating a complete globular domain escape virus by 12 sequential individual mAb-selection steps (we refer to this virus as S12)[15], in which each amino acid substitution in the escape virus epistatically altered the functionality of additional HA substitutions.

[1]Laboratory of Viral Diseases, National Institute of Allergy and Infectious Diseases, National Institutes of Health, Bethesda, Maryland, USA. [2]Department of Medicine, Vanderbilt University School of Medicine, Nashville, Tennessee, USA. [3]Vaccine Research Center, National Institute of Allergy and Infectious Diseases, National Institutes of Health, Bethesda, Maryland, USA. Correspondence should be addressed to J.W.Y. (jyewdell@mail.nih.gov).

Received 19 September 2016; accepted 3 January 2017; published online 13 February 2017; doi:10.1038/ni.3680

Consequently, we used mixtures of mAbs specific for a common antigenic site in an iterative sequential process. After multiple rounds of mAb selection, we obtained a panel of viruses that shared common amino acid substitutions for the Sb (with one exception), Ca1, Ca2 and Cb sites, but with unique amino acid substitutions for the Sa site (**Supplementary Table 1**). For the Sb, Ca1 and Ca2 sites, a single amino acid substitution was sufficient to ablate the binding of a large fraction of representative site-specific mAbs. By contrast, the Sa and Cb sites required three and four amino acid substitutions, respectively.

To define the antigenicity of these viruses in detail, we used a panel of 62 well-characterized mAbs that are specific for the known antigenic sites (by ELISAs) (**Fig. 1b**)[10,15]. The results showed that the Δ4 viruses maintaining the wild-type (WT) Sa (SaΔ4 virus), Sb (SbΔ4 virus) or Cb (CbΔ4 virus) sites were largely recognized only by mAbs specific for their cognate antigenic site while demonstrating greatly reduced affinity with nearly all of the mAbs specific for the four altered sites. Not unexpectedly, given the intimate structural proximity of the Ca1 and Ca2 sites, it proved most difficult to completely abrogate the reciprocal reactivity of the Ca1-specific and Ca2-specific mAbs on the Ca1Δ4 or Ca2Δ4 viruses.

We further validated the predicted antigenicities of the Δ4 viruses in the panel by using polyclonal guinea pig (GP) serum raised to PR8. We depleted GP serum antibodies by incubation with WT PR8, each of the Δ4 viruses, S12, or, as a negative control, an influenza B virus (IBV). To minimize steric interference between antibodies that bind to distinct antigenic sites, we then generated antigen-binding Fab fragments from five representative mAbs (one per antigenic site) and used the depleted sera to compete for their binding in ELISAs. Adsorbing GP sera with either S12 or IBV failed to remove Abs that could compete with any of the Fabs examined (**Supplementary Fig. 1a**). As expected, incubation with PR8 (as a positive control) removed nearly all of the competing Abs for each of the Fabs, except for the Ca2-specific Fab. Adsorption of the GP serum with each of the Δ4 viruses selectively removed Abs that competed with the cognate Fab. Notably, for the Ca2Δ4 and Ca1Δ4 viruses adsorption actually increased the binding of the cognate Fabs. This is explained by previous findings showing that binding of Sa-specific Abs enhances the binding of Ca-specific Abs[16]. Thus, in the absence of competing Ca-specific Abs, the remaining Sa-specific Abs likely enhanced anti-Ca Fab binding, extending the enhancement phenomenon to serum Abs.

On the basis of these findings we conclude that the antigenic sites in the panel of Δ4 viruses are sufficiently well resolved to use the panel to characterize B cell and Ab ID.

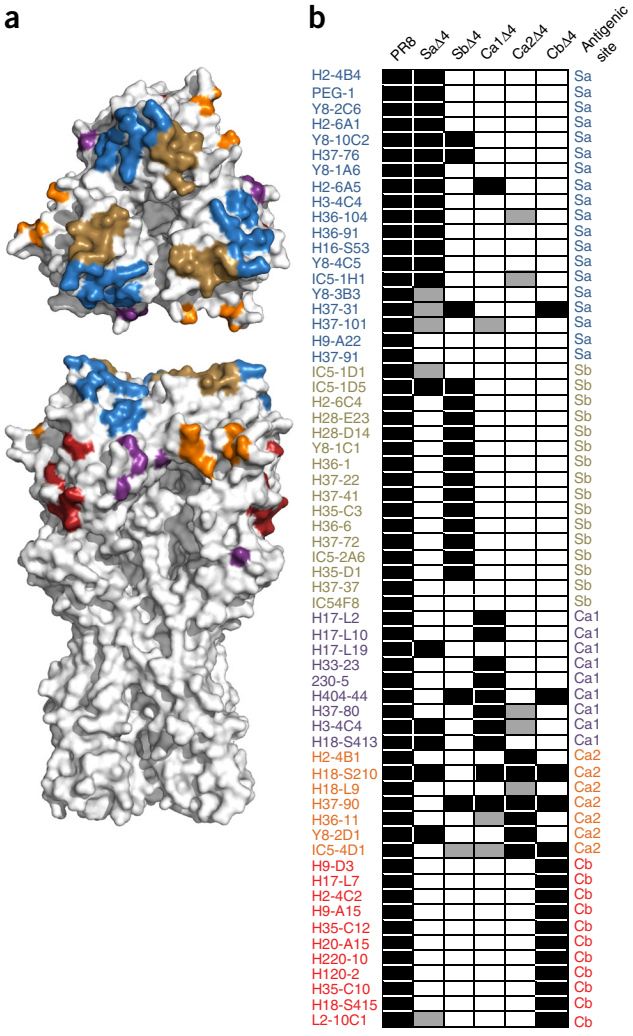

Figure 1 Characterization of Δ4 viruses. (**a**) Crystal structure of PR8 HA (PDB ID 1RUZ)[43] viewed from the top and side, with the five major globular-domain antigenic sites in color (Sa, blue; Sb, gold; Ca1, purple; Ca2, orange; Cb, red). (**b**) Antigenicity of the Δ4 viruses, as assessed by measuring the relative binding affinity by ELISA with a panel of 62 well-characterized mAbs. Black boxes indicate similar affinity to the parental PR8 virus; gray boxes indicate >2-fold but <10-fold reduction in K_D values; and white boxes indicate >10-fold reduction in K_D values.

B cell immunodominance hierarchy is dynamic and well ordered

We next used the Δ4 virus panel to investigate ID for B cell responses in mice that were infected intranasally (i.n.) with PR8. Extrafollicular B cells respond rapidly to IAV in the draining mediastinal lymph nodes (MLNs)[17–19]. We first measured responses using enzyme-linked immunospot (ELISPOT) assays to enumerate Ab-secreting cells (ASCs) at various times after infection. We used recombinant HA proteins (rHA) matching the HAs encoded by the Δ4 viruses as ELISPOT probes to determine the site specificity of the response. ASCs that respond immediately are most probably short-lived plasma cells that comprise the immediate helper T cell– and germinal center (GC)-independent response[18,19]. By day 14, ASCs are mostly derived from early diversified and affinity-matured GC B cells[20].

ELISPOT analysis of MLNs showed the expected rapid increase in the number of ASCs between days 3 and 7 (**Fig. 2a**). Cb-specific B cells dominated the early response (**Fig. 2a**), consistent with early findings using hybridomas[12]. Low numbers of B cells specific for each of the other sites were detected at day 7 but not at day 9; the numbers of ASCs then recovered, with Sb-specific ASCs outnumbering ASCs specific for the Sa, Ca1 or Ca2 sites.

By 14 d post infection (d.p.i.) humoral responses are dominated by rapidly dividing GC-derived B cells, which, in addition to their numerical advantage relative to extrafollicular B cells, secrete affinity-matured Abs. Unlike plasma cells, GC B cells have appreciable amounts of cell surface immunoglobulin, enabling their flow cytometric characterization using fluorescently labeled antigens (**Supplementary Fig. 2a**).

We quantified GC B cells using rHA probes (which possess an additional mutation in the sialic acid binding site (Tyr98Phe) to abolish HA binding to cell surface sialic acids (**Supplementary Fig. 2b**))[21]. Each of the rHA probes bound to GC B cells from mice that had been infected with PR8 (positive control) but did not bind to GC B cells from

mice that had been infected with J1 (negative control; a re-assortant PR8-Hong Kong/68 (H3N2) virus that contains the H3 HA gene segment with seven PR8 gene segments), demonstrating their specificity (**Supplementary Fig. 2c**).

By analyzing MLN GC B cells from PR8-infected mice at 14, 21 and 28 d.p.i., we found that Cb-specific B cells dominated on days 14 and 21 (**Fig. 2b**). On day 14, only Sa-specific B cells were also present at levels substantially greater than the frequencies observed using S12 rHA, which we used to set background frequencies for identifying globular-domain-specific B cells. By day 28, the numbers of B cells that were specific for each of the four other sites approached the numbers of Cb-specific B cells. The sum of each of the specificities on each day was similar to the total HA response measured using WT PR8 HA to stain cells (**Supplementary Fig. 2d**), supporting the validity of using the Δ4 virus panel to quantify ID.

These findings showed that Cb responses rapidly emerged in both extrafollicular and GC B cells. After several rounds of affinity maturation and GC selection, the GC response became more diversified, with broader specificity.

Lymph node B cells predict serum Ab immunodominance

We previously reported that the average affinity of GC B cells for HA predicts the affinity of the anti-HA serum Ab response[22]. To examine how the specificity of anti-HA GC B cells predicted serum response, we measured site-specific serum polyclonal Ab (pAb) responses (in ELISAs) using purified HA from the WT and Δ4 viruses as antigens and a κ chain–specific secondary Ab to detect both IgG and IgM. Binding to S12 HA defined the background level of stem-specific and noncanonical globular-domain-binding Abs to a nearly completely drifted HA globular domain. Anti-HA titers increased 2.5-fold between days 14 and 40 after i.n. infection (**Fig. 2c**). Consistent with our quantification of ASCs and GC B cells, the titers of Cb-specific Abs rose quickly after infection, attaining near-maximum levels by 14 d.p.i (**Fig. 2c**). On day 14, we barely detected Abs specific for the other sites. Of these, the titers of Sb-specific Abs were the first to increase (**Fig. 2c**), nearly reaching Cb-specific Ab titers 1 week later; the titers then surpassed the Cb-specific Ab titers after another week and maintained ID at day 40 (**Fig. 2c**). Sa-specific and Ca2-specific Abs were first detected on day 28, and these continued to increase on day 40 (**Fig. 2c**). Ca1-specific Abs were detected above background values on only day 40. The cumulative response toward the five antigenic sites was close to the response to WT PR8, further corroborating our ability to dissect ID with the panel of Δ4 viruses (**Fig. 2d**). We did not detect antigenic-site-specific differences in the isotype composition of the Abs; IgM constituted 25% of the Abs at day 14, and its titers progressively waned thereafter (**Supplementary Fig. 3**).

Although B cells specific for the Sa- and Sb-sites were higher and lower, respectively, at earlier times than serum Ab levels, in general, we measured a strong positive correlation between the frequency of antigen-specific GC B cells and serum Ab levels (**Fig. 2e**). Thus, as with Ab affinity[22], the numbers of follicular GC B cells in the draining LN accurately predicted the subsequent serum response, consistent with proximal LN GC B cells being the primary source of Ab once they became ASCs after migrating from the immune organs.

Parallel analysis performed on splenic GC B cells showed that the overall ID pattern was similar, particularly on day 14, when Cb-specific B cells were highly dominant (all other specificities were at S12 background values) (**Supplementary Fig. 4a**). At later times, however, the pattern was clearly distinct from that of the MLN, with Sa-specific B cells moving up in the hierarchy relative to the B cells

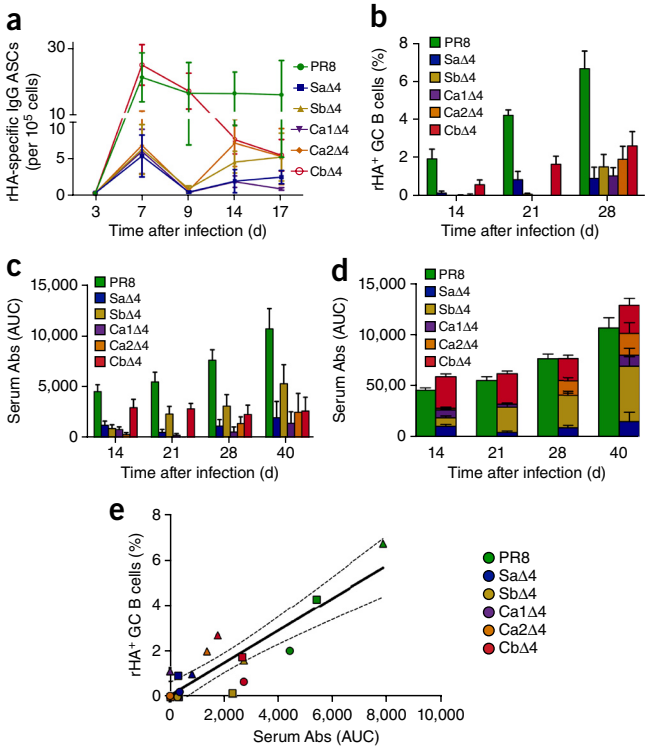

Figure 2 B cell kinetics and Ab immunodominance after IAV infection. We infected C57BL/6 mice i.n. with 50 half-maximal tissue-culture infectious dose ($TCID_{50}$) of PR8. (**a**) ELISPOT assays with cells from the MLN using rHA derived from the different Δ4 viruses at the indicated time points ($n = 3$ individual mice per group for every experiment). (**b**) Frequency of antigenic-site-specific GC B cells over time (MLNs from $n = 5$ animals were pooled per experiment). Frequencies of S12-specific GC B cells were considered to be baseline values and were subtracted from the values obtained with the PR8 and Δ4 viruses. (**c**) ELISA-based quantification of concentrations of Abs specific for the HAs of the PR8 and Δ4 viruses from serum collected at 14, 21, 28 and 40 d.p.i. ($n = 10$ mice per group). AUC values derived from infection with S12 were considered to be baseline values and were subtracted from the AUC values obtained with the PR8 and Δ4 viruses. (**d**) Cumulative serum Ab response. After subtraction of the S12 AUC value, the sum of the response to the five antigenic sites was almost equal to the anti-PR8 response. (**e**) Scatter plot showing the correlation between recognition of the different HAs (as in **c**), as determined by ELISA, and frequency of GC B cells (as in **b**) (Pearson $r = 0.8814$). Circles represent values at 14 d.p.i., squares represent values at 21 d.p.i., and triangles represent values at 28 d.p.i. Dashed lines represent 95% confidence intervals. Data are from the average of three (**a**,**b**) or two (**c**) independent experiments (average ± s.e.m. for **a**–**d**). $P < 0.0001$ (Pearson correlation; **e**).

specific for the other sites. Most notably, there was a poor correlation between the splenic GC B cell ID hierarchy and serum Ab responses (**Supplementary Fig. 4b**), suggesting that most of the Abs arose from B cells originating in proximal LNs.

When considering total number of HA-binding GC B cells rather than their frequency, we observed the same phenomenon, with a strong positive correlation of serum Ab levels with MLN cell numbers but not splenic cell numbers (**Supplementary Fig. 4c,d**). Notably, the total number of rHA-binding cells (from the spleen and MLN) also correlated well with serum Ab levels (**Supplementary Fig. 4e**). Taken together, these data strongly implied that B cells originating in the draining LN GCs were the principal source of serum Abs.

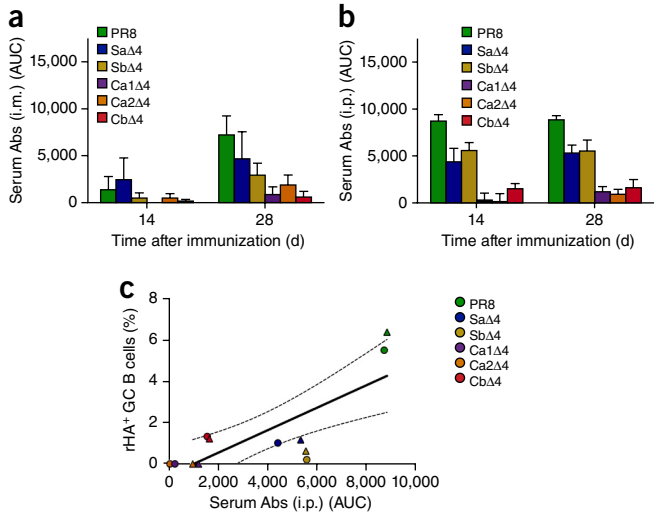

Figure 3 Intraperitoneal and intramuscular immunizations elicit similar Ab immunodominance patterns distinct from that in response to infection. (**a**,**b**) Concentrations of serum Abs to the PR8 and Δ4 viruses in mice that were immunized intramuscularly with 6 μg of UV-inactivated virus with Titermax adjuvant ($n = 6$ mice per group) (**a**) or intraperitoneally with 2,500 hemagglutination units (HAU) of UV-inactivated PR8 ($n = 8$ mice per group) (**b**). AUC values for the S12 virus were considered to be baseline and were subtracted from values obtained with the PR8 and Δ4 viruses. (**c**) Scatter plot showing correlation between the frequency of splenic GC B cells and ELISA recognition of the different HAs (as in **b**) (Pearson $r = 0.7926$). Circles are 14 d after immunization, and triangles are 28 d after immunization. Dashed lines represent 95% confidence intervals. Data are from the average of two independent experiments (**a**,**b**) or the average from three independent experiments for which three spleens were pooled (**c**) (average ± s.e.m. for **a**,**b**). $P = 0.0021$ (Pearson correlation; **c**).

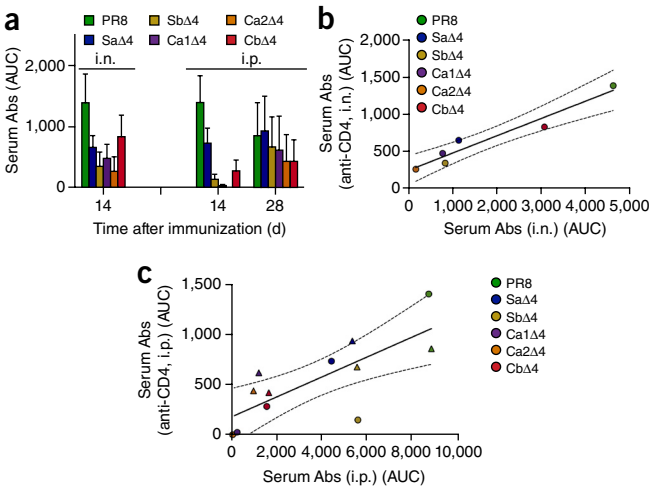

Figure 4 CD4+ T cells positively modulate the magnitude and duration of Ab responses but not their immunodominance. We depleted CD4+ T cells by administering GK1.5 mAb by i.p. injection 1 d before infection or immunization, and subsequently on every third day. We challenged mice by i.n. infection with 50 $TCID_{50}$ of PR8 or by i.p. injection with 2,500 HAU of UV-inactivated-PR8. (**a**) Serum Abs to the HAs from the PR8, D4 and S12 viruses at day 14 and 28 after infection (i.n.) or immunization (i.p.) ($n = 10$ mice per group). AUC values for the S12 virus were considered to be baseline and were subtracted from values obtained with the PR8 and Δ4 viruses. (**b**,**c**) Scatter plots showing correlation between serum Abs recognizing the different HAs in regular mice (as in **Figs. 2c** and **3b**) and those in CD4-depleted mice (as in **a**) for i.n. infection (**b**) or i.p. immunization (**c**) (Pearson $r = 0.7623$). Circles represent 14 d, and triangles 28 d, after infection or immunization. Dashed lines represent 95% confidence intervals. Data are from the average of two independent experiments (average ± s.e.m.) (**a**). $P = 0.0039$ (Pearson correlation; **b**,**c**).

Vaccination alters the immunodominance hierarchy

A critical practical question is how vaccination and infection differ in eliciting protective immunity. We immunized mice once via intramuscular (i.m.) or intraperitoneal (i.p.) injection with purified PR8 that we had UV-irradiated sufficiently to reduce *de novo* synthesis of viral proteins in infected cultured cells to undetectable levels. We co-formulated the virus injected intramuscularly with Titermax Gold adjuvant. We then measured site-specific serum Abs and MLN and splenic GC B cells on days 14 and 28 after immunization.

Intraperitoneal immunization gave a more rapid response, with i.m. immunization yielding low serum Ab titers on day 14 (**Fig. 3a**,**b**). At day 28, serum Ab titers from i.p.-injected mice were unchanged, whereas titers from i.m.-injected mice increased to levels that nearly matched those of the i.p.-injected mice (**Fig. 3a**,**b**). Notably, the day 28 serum Ab response to vaccination was actually greater than the response following i.n. infection (**Figs. 2c** and **3a**,**b**). Although responses to i.n. infection, and i.m. and i.p. immunization were of similar magnitude, there were notable differences in the ID hierarchy.

With vaccination-elicited Abs, we did not observe the highly dynamic changes in the ID hierarchy we saw following infection. Furthermore, the majority of the Abs targeted the Sa and/or Sb antigenic sites, but not the Cb site, at both day 14 and day 28 (**Fig. 3a**,**b**). We measured the frequency of splenic GC cells specific for each antigenic site 14 or 28 d after i.p. injection and found a strong correlation between the frequency of GC cells and the serum response (**Fig. 3c**), suggesting that splenic B cells were a major source of serum Abs following i.p. injection. The correlation of serum Ab levels with Sa-specific and Sb-specific B cells was not as robust, suggesting that these B cells might have preferentially generated rapidly proliferating, short-lived ASCs. Peritoneal lymph has been reported to drain mostly to the MLNs[23], but our data suggested that some peritoneal antigens could traffic equally well to the spleen. Indeed, analysis of MLNs at 14 d.p.i. showed a near-perfect correlation between splenic and MLN GC B cell frequencies (**Supplementary Fig. 3f**).

Taken together, these findings clearly showed that the ID hierarchy was greatly influenced by the form of antigen and route of administration and was not rigidly dictated by a uniform lymphoid B cell repertoire.

CD4+ T cells do not influence immunodominance

To study the influence of CD4+ T cell–mediated help on the ID hierarchy of the HA-specific Abs, we challenged CD4-depleted mice by i.n. infection or i.p. immunization (**Fig. 4**). As reported previously[24,25], we found that CD4+ T cells were necessary for high and sustained anti-HA serum Ab titers (**Fig. 4**). Indeed, at day 28, we barely detected anti-HA serum Abs after i.n. infection (data not shown). Although serum Ab responses were more durable after i.p. immunization, titers diminished and did not increase similarly to that observed when CD4+ T cells were present (**Fig. 4a**). Following either infection or immunization, T cell depletion prevented GC formation, as determined by the absence of B cells with GC markers that could be detected by both flow cytometry and immunofluorescence of frozen MLN (infection) or spleen sections (immunization) (**Supplementary Fig. 5**).

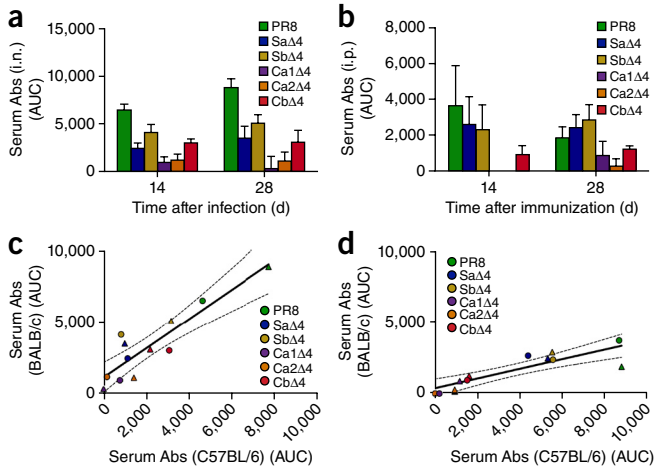

Figure 5 Ab immunodominance varies between mouse strains. (**a**,**b**) ELISAs for recognition of the HAs from the PR8 and Δ4 viruses in the sera of BALB/c mice at 14 and 28 d after i.n. infection with 50 $TCID_{50}$ PR8 ($n = 8$ mice per group) (**a**) or i.p. immunization with 2,500 HAU of UV-inactivated-PR8 ($n = 6$ mice per group) (**b**). AUC values for the S12 virus were considered to be baseline and were subtracted from values obtained with the PR8 and Δ4 viruses. (**c**) Scatter plot showing the correlation for ELISA-based recognition of the different HAs between Abs from C57BL/6 (as in **Fig. 2c**) and BALB/c (as in **a**) mice after i.n. infection (Pearson $r = 0.9027$). (**d**) Scatter plot showing the correlation ELISA-based recognition of the different HAs between Abs in C57BL/6 (as in **Fig. 3b**) and BALB/c (as in **b**) mice after i.p. immunization (Pearson $r = 0.8684$). In **c**,**d**, circles represent values 14 d after infection or immunization, and triangles represent values 28 d after infection or immunization. Dashed lines represent 95% confidence intervals. Data are from the average of two (**a**,**b**) independent experiments (average ± s.e.m.). $P = 0.0001$ (**c**) or $P = 0.0002$ (**d**) (Pearson correlation).

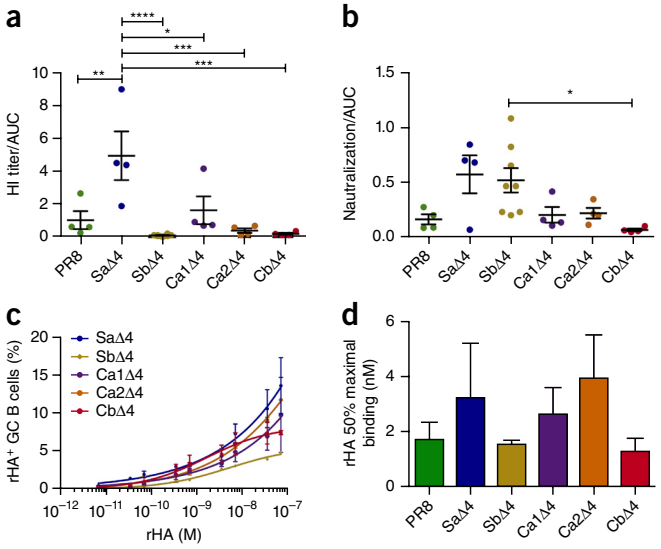

Figure 6 Abs directed to different antigenic sites show distinct functionalities. (**a**,**b**) Ratio between the HI (**a**) or microneutralization (MN) (**b**) end point titer and the ELISA reactivity toward PR8 HA in mice 21 d after i.n. infection with 50 $TCID_{50}$ of S12, PR8, or a Δ4 virus ($n = 4$ for the PR8, Sa, Ca1 and Ca2 groups; $n = 5$ for the Cb group; $n = 8$ for the Sb group). Higher values represent higher serum efficacy. (**c**,**d**) Titration curves of MLN GC B cells to rHA from PR8 following i.n. infection with Δ4 viruses (**c**) and rHA concentration necessary to reach 50% of the maximal binding was calculated for each titration curve (**d**). Data are representative of one biological experiment with four technical replicates per sample (**a**,**b**) or are from the average of two independent experiments (**c**,**d**) (mean ± s.e.m. for **a**–**d**). $^{*}P < 0.05$, $^{**}P < 0.01$, $^{***}P < 0.001$ and $^{****}P < 0.0001$ (one-way analysis of variance with *post hoc* Tukey's multiple-comparison test; **a**,**b**).

Despite ablating GCs and compromising serum Ab responses, depleting $CD4^+$ T cells had little effect on the ID hierarchy following i.n. infection or i.p. immunization (**Fig. 4a**,**b**). By plotting the responses elicited without treatment and after $CD4^+$ T cell depletion, we found an excellent correlation; $CD4^+$ T cell depletion had a greater effect on ID following i.p. immunization, particularly on day 14 at which time point responses to Sa dominated and those to Sb were diminished (**Fig. 4c**). However, the overall correlation with serum Abs from untreated mice was still robust (**Fig. 4c**). These findings showed that although $CD4^+$ T cell help was necessary for high and durable Abs titers, it was not a major modulator of the ID hierarchy.

Stem-specific antibodies are present at low titers

To measure the fraction of serum Abs specific for the conserved stem region of HA, we used a chimeric virus with an antigenically shifted head (H5) and the PR8 stem[26] and examined nearly all of the sera described above, using ELISA (**Supplementary Table 2**). As expected, after a single i.n. infection, we could detect stem-specific serum Abs at only low titers, which, notably, did not increase with time. Similarly, neither i.p. nor i.m. immunization generated robust anti-stem responses, although in both cases the titers increased with time (**Supplementary Table 2**); the early response to i.m. immunization, although weak, represented a substantial fraction of the globular-domain response (**Supplementary Table 2**). $CD4^+$ T cell depletion slightly decreased the stem-specific Ab responses. Anti-stem responses were modestly increased by intraperitoneal challenge after i.n. infection. Thus, as expected, stem-specific Ab responses were not strongly induced in primary immune responses or after a single challenge immunization.

Mouse genetic background influences immunodominance

To examine the extent to which C57BL/6 and BALB/c mice differ in their B cell ID hierarchies, we examined serum Abs in BALB/c mice at 14 and 28 d following i.n. infection or i.p. immunization (**Fig. 5a**,**b**). The Cb-specific Ab response to i.n. infection was of similar magnitude in BALB/c and C57BL/6 mice on 14 and 28 d.p.i. (**Fig. 5a**); however, it descended one rung in the ID ladder, due to the ascension of Sb-specific Abs, which were dominant at both time points. Furthermore, the early Sa-specific Ab response was much more robust, and even surpassed the Cb-specific response observed at 28 d.p.i. (**Fig. 5a**). We also observed a slightly higher Ca2-specific Ab response at 14 d in BALB/c mice than in C57BL/6 mice, in which they were not detected above background values (**Fig. 5c**). After i.p. immunization, Sa-specific and Sb-specific Abs dominated from the initial time points, and the pattern did not change after 28 d, similarly to that in C57BL/6 mice (**Fig. 5d**). Thus, there were differences in the ID hierarchies in BALB/c and C57BL/6 mice, particularly in the early response following i.n. infection.

Polyclonal antibodies show antigenic-site-specific functions

Our findings showed that there was a highly reproducible and dynamic HA antigenic-site-specific ID hierarchy in Ab responses following IAV infection or vaccination. To understand the functional consequences of the differential responses to the antigenic sites, we infected mice with each Δ4 virus and collected sera at 21 d.p.i for testing in ELISA,

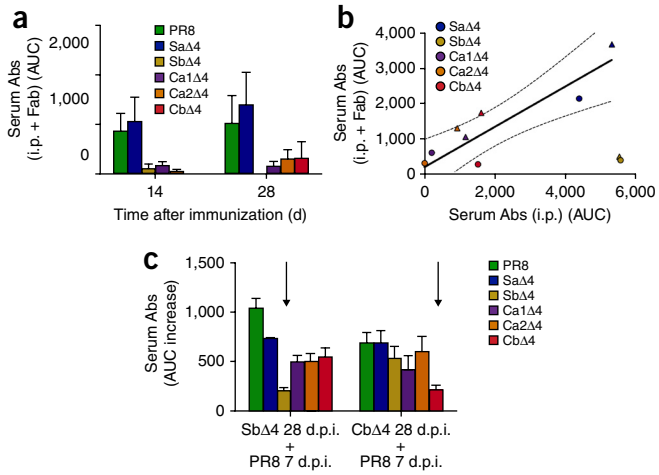

Figure 7 Pre-existing Abs influence immunodominance in recall responses. (**a**) Levels of Abs specific for the HAs from the PR8, S12 and Δ4 viruses 14 d and 28 d after i.p. immunization with 2,500 HAU of UV-inactivated PR8 premixed with Fabs from H28-E23, a Sb-site-specific mAb, after subtraction of Ab levels at day 1 after immunization (internal experimental baseline) ($n = 5$ mice per group). AUC values for the S12 virus were considered to be baseline and were subtracted from values obtained with the PR8 and Δ4 viruses. (**b**) Scatter plot showing correlation of serum Ab recognition of the different HAs after i.p. immunization (as in **Fig. 3b**) versus that after i.p. immunization with virus + Fab (in **a**). Besides the PR8- and Sb-specific responses, the general ID pattern was maintained (Pearson $r = 0.8684$; calculated excluding the Sb points). Circles represent Ab levels 14 d after immunization, and triangles represent Ab levels at 28 d after immunization. Dashed lines represent 95% confidence intervals. (**c**) Challenge experiment. Serum Ab levels to the PR8, S12 and Δ4 viruses 7 d after i.p. challenge with 2,000 HAU of PR8, which was done at day 28 after i.n. infection with 50 $TCID_{50}$ SbΔ4 or CbΔ4 virus ($n = 6$ mice per group). Shown is the AUC after subtracting the 28-d.p.i. response. Arrows indicate the site corresponding to the primary virus. Data are from the average of one independent experiment with three technical replicates (**a**) or of two independent experiments (**c**) (average ± s.e.m. for **a**,**c**). $P = 0.0036$ (Pearson correlation; **b**).

hemagglutination inhibition (HI) and virus neutralization (VN) assays. By normalizing HI or VN titers to the ELISA 'area under the curve' (AUC) titer, we were able to assess the specific antiviral activity of the pAbs specific to each antigenic site (**Fig. 6a**,**b**).

As predicted from previous unpublished studies with mAbs (**Supplementary Table 3**, and J.W.Y. and W. Gerhard, unpublished data), Cb-specific pAbs showed the lowest specific activities in HI and VN assays, whereas Sa-specific pAbs had high specific activities in both assays (**Fig. 6a**,**b**). Sb-specific pAbs demonstrated high activity in VN assays, as previously observed for Sb-specific mAbs. Unexpectedly, however, in HI assays the specific activity of Sb-specific pAbs was even lower than that of Cb-specific pAbs (**Fig. 6a**).

To investigate whether Ab avidity could explain the site-dependent functional differences, we used our newly developed method that allows determination of average B cell population avidity[22]. This method is based on graded flow cytometric staining of GC B cells with fluorescent rHA to calculate the AC_{50} value, the concentration of rHA that stains 50% of GC B cells, which closely tracks the affinity of serum Abs[22]. We used rHA from WT PR8 to stain GC cells from mice that were infected with each of the Δ4 viruses (**Fig. 6c**). A large fraction of PR8-binding Abs in these mice were specific for the preserved antigenic site (**Supplementary Fig. 6**). AC_{50} measurements revealed that B cells specific for each of the sites generated Abs with a high average affinity, with corresponding dissociation constants ranging from 1.4 nM to 4 nM (**Fig. 6d**). These findings demonstrated that there could be small but substantial differences in Ab affinity at the level of antigenic sites. This difference did not, however, account for the site-specific functional differences in pAbs in the VN and HI assays. Although Cb-specific GC B cells had the highest average affinity, Cb-specific pAbs had the lowest functional activities. Thus, we attribute the site-specific functional differences to the disposition of the antigenic sites on the HA trimer and not to the affinities of Abs elicited.

Modulation of immune responses

A critical complexity of influenza vaccinations in humans is the effect of pre-existing Abs on subsequent responses. With the exception of young children, virtually everyone vaccinated with IAV has been previously infected and/or vaccinated with IAV. To examine the influence of competing Abs on vaccination, we vaccinated mice intraperitoneally with UV-inactivated PR8 virus mixed with high-affinity Fab fragment ($K_D = 45$ nM) of the H28-E23 Sb-specific mAb. We used a Fab fragment to avoid potential complications of altering antigen presentation or processing owing to Fc-mediated uptake or to association with complement and other serum proteins. We found that by including the H28-E23 Fab in the vaccine, the overall anti-HA response at both days 14 and 28 was decreased by ~5-fold (**Fig. 7a**). Remarkably, although the Sb-specific response was almost completely suppressed, the ID hierarchy was otherwise similar on both days (**Fig. 7a**,**b**). Because the anti-Sb response is normally dominant on day 28, this indicates that Sb-specific B cells do not 'immunodominate' other specificities, as is often observed in $CD8^+$ T cell responses[27,28].

To extend these findings to a more physiological setting, we infected mice i.n. with either SbΔ4 or CbΔ4 and 28 d later challenged them via i.p. vaccination with UV-inactivated WT PR8. We chose these viruses because their cognate preserved sites were immunodominant on day 28. Seven days after challenge, we measured the ID hierarchy among serum Abs via ELISA (**Supplementary Fig. 7**).

The results partially recapitulated the Fab experiment data; we found selective suppression of Ab responses to the previously immunized antigenic site but, in this protocol, also an augmented response to the drifted sites (**Fig. 7c**). Neither approach induced detectable anti-stem titers (**Supplementary Table 2**). This finding helps explain the great variability observed in the phenomenon of original antigenic sin (OAS), in which virus administration route, order of administration and timing of re-challenge all have a key role in OAS induction[29].

DISCUSSION

The ability to rationally focus vaccine-induced Ab responses onto targeted antigenic sites requires deeper understanding of Ab ID, with the first step being characterization of the B cell and Ab ID hierarchies. By selecting a panel of IAV escape mutants that maintain antigenicity in one of five HA globular domain antigenic sites, we explored the responses at the level of individual antigenic sites.

By dissecting GC B cell and Ab ID, we found that Cb-specific B cells dominated the immediate response following infection, extending hybridoma-based findings[12,13,30]. A previous study reported that B cells expressing nearly germline immunoglobulin of a single idiotype (specific for Cb)[12] dominated early extrafollicular, and later follicular, B cell responses[18]. Extrafollicular B cells may account for the serum Abs to the Sb, Ca1 and Ca2 sites on day 14, given the low frequency of corresponding GC B cells.

At 21 d.p.i., we detected a strong Sb-specific GC B cell response. Over the next 2 weeks, the Sa-specific and Ca2-specific responses rose, and Ca1 responses were detected only weeks later. Notably,

serum Ab levels and LN GC B cell frequencies strongly correlated, suggesting that GC-originating B cells provided a substantial fraction of serum Abs and implying that there were small differences in the average proliferative capacities or Ab-secretion rates between the GC B cell progeny once they left the LN.

We found clear differences in the ID hierarchies of C57BL/6 versus BALB/c mice. The extent to which this was due to differences in immunoglobulin-encoding genes versus other genetic or epigenetic (for example, microbiota) factors remains a key question that could be addressed by using the large panel of inbred mouse strains generated by the collaborative cross project[31]. From this finding, we predict significant differences in the ID hierarchy in individual humans, no doubt enhanced by environmental factors, not least of which is the history of previous infections with IAV[32].

Notably, the ID hierarchies in infected animals versus animals immunized with inactivated virus differed markedly. After i.m. injection with adjuvant, Sa-specific Abs dominated the response at day 14 and day 28, with Sb-specific Abs making a major contribution at day 28. Following i.p. immunization, Sa-specific and Sb-specific Abs dominated the responses at days 14 and 28. Because splenic GC B cell frequencies correlated well with the serum responses, we could not attribute these to intrinsic differences in B cell precursor frequencies but rather to the mode of antigenic delivery to the spleen. For responses at later time points, GCs persisted far longer following infection[18,22,33,34] versus immunization[35,36], which may have contributed to the time-dependent diversification of responses after infection. Residual antigen presentation following i.n. infection could also have contributed to the continuous diversification of the repertoire specificity[37].

We confirmed previous findings that B cells could respond to IAV infection in the absence of T cell help, but with diminished and much more transient serum Ab responses[24,25]. We showed that eliminating $CD4^+$ T cells (and consequently GCs) had little effect on the ID hierarchy following either i.n. infection or i.p immunization. This is consistent with the idea that ID hierarchy is initially governed by intrinsic properties of the B cell repertoire and the mechanism of antigen delivery or presentation to the B cell compartment.

Analysis of the pAbs induced by the Δ4 viruses (normalizing responses to the ELISA titers) recapitulated previous results (J.W.Y. and W. Gerhard, unpublished data) showing that Sa-specific, Sb-specific and Ca1-specific mAbs exerted the highest VN activities, Cb-specific mAbs exerted the least and Ca2-specific mAbs were intermediate (**Supplementary Table 3**). Based on AC_{50} analysis of GC B cells, this could not be attributed to differences in Ab affinity. A simple explanation for these findings is that epitope proximity to the sialic acid receptor site governs *in vitro* neutralization efficiency.

Antigenic-site-specific serum HI activity mostly paralleled the VN results, with the unexpected observation being that Sb-specific Abs showed low specific activity, in distinct contrast to that for mAbs. Whatever the mechanism, this shows that site-specific differences in polyclonal functional assays may not be revealed at the level of mAbs, underscoring the importance of tackling Ab function in the natural polyclonal serum environment.

Finally, we found that after immunogen re-challenge, Abs selectively suppressed responses to the cognate antigenic site, enabling B cells specific for nondominant sites to rise in the ID hierarchy. This is the opposite of the phenomenon of OAS, in which immune responses are heavily skewed toward determinants shared by the challenge and priming viruses[38]. It is not unprecedented, however, with recent studies showing that the conditional nature of OAS[29,39] and pre-existing human Ab levels negatively correlate with boosting responses to the same strain[40,41]. Ultimately, the strength of OAS may be governed by the balance of Abs versus the numbers of their cognate memory B cells. With high Ab levels, responses are suppressed; with low Ab levels, memory B cells dominate naive B cells. Our findings indicate that, when using a single immunogen, responses can be focused on various domains by including an appropriate antibody or antibody-like molecule[42] that sterically prevents Ab access to a given antigenic site if relevant memory cells are present.

METHODS

Methods, including statements of data availability and any associated accession codes and references, are available in the online version of the paper.

Note: Any Supplementary Information and Source Data files are available in the online version of the paper.

ACKNOWLEDGMENTS

We thank the NIAID Comparative Medicine Branch for maintaining the mice used in this study, and P. Palese and F. Krammer (Icahn School of Medicine at Mount Sinai) for the chimeric HA virus construct. Supported by the Division of Intramural Research, National Institute of Allergy and Infectious Diseases (J.W.Y. and A.B.M.).

AUTHOR CONTRIBUTIONS

D.A. designed and performed experiments, analyzed data and wrote the paper; J.S.G., M.A., I.K., H.D.H., G.M.F. and S.R.D. designed and performed experiments and analyzed data; A.K.W., M.P., D.J.L. and A.B.M. designed and generated critical reagents for the study; and J.W.Y. designed experiments, analyzed data and wrote the paper. All authors provided useful comments on the manuscript.

COMPETING FINANCIAL INTERESTS

The authors declare no competing financial interests.

1. Yewdell, J.W. Confronting complexity: real-world immunodominance in antiviral $CD8^+$ T cell responses. *Immunity* **25**, 533–543 (2006).
2. Krammer, F. & Palese, P. Advances in the development of influenza virus vaccines. *Nat. Rev. Drug Discov.* **14**, 167–182 (2015).
3. Burton, D.R., Poignard, P., Stanfield, R.L. & Wilson, I.A. Broadly neutralizing antibodies present new prospects to counter highly antigenically diverse viruses. *Science* **337**, 183–186 (2012).
4. Wheatley, A.K. & Kent, S.J. Prospects for antibody-based universal influenza vaccines in the context of widespread pre-existing immunity. *Expert Rev. Vaccines* **14**, 1227–1239 (2015).
5. Victora, G.D. & Wilson, P.C. Germinal center selection and the antibody response to influenza. *Cell* **163**, 545–548 (2015).
6. Hutchinson, E.C. *et al*. Conserved and host-specific features of influenza virion architecture. *Nat. Commun.* **5**, 4816 (2014).
7. Reading, S.A. & Dimmock, N.J. Neutralization of animal virus infectivity by antibody. *Arch. Virol.* **152**, 1047–1059 (2007).
8. Altman, M.O., Bennink, J.R., Yewdell, J.W. & Herrin, B.R. Lamprey VLRB response to influenza virus supports universal rules of immunogenicity and antigenicity. *eLife* **4**, e07467 (2015).
9. Caton, A.J., Brownlee, G.G., Yewdell, J.W. & Gerhard, W. The antigenic structure of the influenza virus A/PR/8/34 hemagglutinin (H1 subtype). *Cell* **31**, 417–427 (1982).
10. Gerhard, W., Yewdell, J., Frankel, M.E. & Webster, R. Antigenic structure of influenza virus hemagglutinin defined by hybridoma antibodies. *Nature* **290**, 713–717 (1981).
11. Yewdell, J.W., Webster, R.G. & Gerhard, W.U. Antigenic variation in three distinct determinants of an influenza type A hemagglutinin molecule. *Nature* **279**, 246–248 (1979).
12. Kavaler, J., Caton, A.J., Staudt, L.M., Schwartz, D. & Gerhard, W. A set of closely related antibodies dominates the primary antibody response to the antigenic site CB of the A/PR/8/34 influenza virus hemagglutinin. *J. Immunol.* **145**, 2312–2321 (1990).
13. McKean, D. *et al*. Generation of antibody diversity in the immune response of BALB/c mice to influenza virus hemagglutinin. *Proc. Natl. Acad. Sci. USA* **81**, 3180–3184 (1984).
14. Staudt, L.M. & Gerhard, W. Generation of antibody diversity in the immune response of BALB/c mice to influenza virus hemagglutinin. I. Significant variation in repertoire expression between individual mice. *J. Exp. Med.* **157**, 687–704 (1983).
15. Das, S.R. *et al*. Defining influenza A virus hemagglutinin antigenic drift by sequential monoclonal antibody selection. *Cell Host Microbe* **13**, 314–323 (2013).

16. Lubeck, M. & Gerhard, W. Conformational changes at topologically distinct antigenic sites on the influenza A/PR/8/34 virus HA molecule are induced by the binding of monoclonal antibodies. *Virology* **118**, 1–7 (1982).
17. Marshall, D., Sealy, R., Sangster, M. & Coleclough, C. T_H cells primed during influenza virus infection provide help for qualitatively distinct antibody responses to subsequent immunization. *J. Immunol.* **163**, 4673–4682 (1999).
18. Rothaeusler, K. & Baumgarth, N. B cell fate decisions following influenza virus infection. *Eur. J. Immunol.* **40**, 366–377 (2010).
19. Sealy, R., Surman, S., Hurwitz, J.L. & Coleclough, C. Antibody response to influenza infection of mice: different patterns for glycoprotein and nucleocapsid antigens. *Immunology* **108**, 431–439 (2003).
20. Baumgarth, N. How specific is too specific? B cell responses to viral infections reveal the importance of breadth over depth. *Immunol. Rev.* **255**, 82–94 (2013).
21. Whittle, J.R. *et al.* Flow cytometry reveals that H5N1 vaccination elicits cross-reactive stem-directed antibodies from multiple Ig heavy-chain lineages. *J. Virol.* **88**, 4047–4057 (2014).
22. Frank, G.M. *et al.* A simple flow-cytometric method measuring B cell surface immunoglobulin avidity enables characterization of affinity maturation to influenza A virus. *MBio* **6**, e01156 (2015).
23. Tsilibary, E.C. & Wissig, S.L. Light and electron microscope observations of the lymphatic drainage units of the peritoneal cavity of rodents. *Am. J. Anat.* **180**, 195–207 (1987).
24. Lee, B.O. *et al.* CD4 T cell–independent antibody response promotes resolution of primary influenza infection and helps to prevent reinfection. *J. Immunol.* **175**, 5827–5838 (2005).
25. Mozdzanowska, K., Furchner, M., Zharikova, D., Feng, J. & Gerhard, W. Roles of $CD4^+$ T cell–independent and T cell–dependent antibody responses in the control of influenza virus infection: evidence for noncognate $CD4^+$ T cell activities that enhance the therapeutic activity of antiviral antibodies. *J. Virol.* **79**, 5943–5951 (2005).
26. Hai, R. *et al.* Influenza viruses expressing chimeric hemagglutinins: globular head and stalk domains derived from different subtypes. *J. Virol.* **86**, 5774–5781 (2012).
27. Bennink, J.R. & Doherty, P.C. The response to H-2-different virus-infected cells is mediated by long-lived T lymphocytes and is diminished by prior virus priming in a syngeneic environment. *Cell. Immunol.* **61**, 220–224 (1981).
28. Jamieson, B.D. & Ahmed, R. T cell memory. Long-term persistence of virus-specific cytotoxic T cells. *J. Exp. Med.* **169**, 1993–2005 (1989).
29. Kim, J.H., Skountzou, I., Compans, R. & Jacob, J. Original antigenic sin responses to influenza viruses. *J. Immunol.* **183**, 3294–3301 (2009).
30. Kavaler, J., Caton, A.J., Staudt, L.M. & Gerhard, W. A B cell population that dominates the primary response to influenza virus hemagglutinin does not participate in the memory response. *Eur. J. Immunol.* **21**, 2687–2695 (1991).
31. Churchill, G.A. *et al.* The Collaborative Cross, a community resource for the genetic analysis of complex traits. *Nat. Genet.* **36**, 1133–1137 (2004).
32. Linderman, S.L. *et al.* Potential antigenic explanation for atypical H1N1 infections among middle-aged adults during the 2013–2014 influenza season. *Proc. Natl. Acad. Sci. USA* **111**, 15798–15803 (2014).
33. Jelley-Gibbs, D.M. *et al.* Unexpected prolonged presentation of influenza antigens promotes CD4 T cell memory generation. *J. Exp. Med.* **202**, 697–706 (2005).
34. Waffarn, E.E. & Baumgarth, N. Protective B cell responses to flu—no fluke! *J. Immunol.* **186**, 3823–3829 (2011).
35. MacLennan, I.C.M. Germinal centers. *Annu. Rev. Immunol.* **12**, 117–139 (1994).
36. Hollowood, K. & Macartney, J. Cell kinetics of the germinal center reaction—a stathmokinetic study. *Eur. J. Immunol.* **22**, 261–266 (1992).
37. Zammit, D.J., Turner, D.L., Klonowski, K.D., Lefrançois, L. & Cauley, L.S. Residual antigen presentation after influenza virus infection affects CD8 T cell activation and migration. *Immunity* **24**, 439–449 (2006).
38. Webster, R.G., Fazekas de St.Groth, S. & Webster, R.G. Disquisition on original antigenic sin. I. Evidence in man. *J. Exp. Med.* **124**, 331–345 (1966).
39. Kim, J.H., Davis, W.G., Sambhara, S. & Jacob, J. Strategies to alleviate original antigenic sin responses to influenza viruses. *Proc. Natl. Acad. Sci. USA* **109**, 13751–13756 (2012).
40. Andrews, S.F. *et al.* High pre-existing serological antibody levels correlate with diversification of the influenza vaccine response. *J. Virol.* **89**, 3308–3317 (2015).
41. Sasaki, S. *et al.* Influence of prior influenza vaccination on antibody and B cell responses. *PLoS One* **3**, e2975 (2008).
42. Fleishman, S.J. *et al.* Computational design of proteins targeting the conserved stem region of influenza hemagglutinin. *Science* **332**, 816–821 (2011).
43. Gamblin, S.J. *et al.* The structure and receptor binding properties of the 1918 influenza hemagglutinin. *Science* **303**, 1838–1842 (2004).

ONLINE METHODS

Animals. C57BL/6 mice were purchased from Taconic Farm. For all experiments, female 8- to 12-week-old mice were used and randomly assigned to experimental groups. All mice were held under specific pathogen-free conditions. All animal procedures were approved and performed in accordance with the NIAID Animal Care and Use Committee Guidelines.

Virus and Δ4 virus selection. Influenza A/Puerto Rico/8/34 (PR8) (Mt. Sinai strain; H1N1) and its mutants were grown in 10-d-old embryonated chicken eggs. Mutants were selected using the Madin–Darby canine kidney (MDCK) culture system as described before[15]. Hybridoma anti-HA Abs were produced as previously described[9,10,14,44]. Briefly, virus was serially diluted 10-fold in a 96-well plate. The combination of mAbs specific for one site at over-neutralizing concentrations was incubated with the virus for 1 h. After incubation for 2 h at 37 °C on MDCK, cells were washed and incubated with selection medium in the presence of mAbs. Viral RNA in the supernatant from cytopathic-effect-positive wells was sequenced. All unique viruses were tested for proper escape, as defined by loss of ELISA reactivity, with a large panel of mAbs. Upon satisfactory escape, the mutant virus was subjected to a second round of selection with mAbs specific for a different site. The procedure was repeated until the Δ4 variants were obtained.

Viral HA purification. Allantoic fluid was clarified by centrifugation, and virus was purified over a sucrose gradient as previously described[8]. For ELISA, purified virus was fractionated by incubation with an equal volume of 15% octyl-β-glucoside. After addition of PBS, the solution was spun at 50,000*g* for 2 h at 4 °C. The supernatant, which contained HA and neuraminidase (NA), was incubated at 56 °C for 30 min after the addition of 10 mM EDTA. The amount of HA in the different viral preparations was normalized by using a combination of methods and was confirmed by immunoblot using a HA_2-specific mAb (data not shown). To further confirm the accuracy of our protein estimation, serum recognition of PR8 and Δ4 HA was directly compared when using virus-purified HA versus rHA probes: the results were remarkably similar, confirming the validity of our estimation (**Supplementary Fig. 1b**).

Infections and immunizations. For i.n. infections, mice were anesthetized with isofluorane and nasally inoculated with 50 $TCID_{50}$ of virus diluted in balanced salt solution (BSS) with 0.1% BSA. For i.p. injections, the virus was UV-inactivated for 4 min on ice and subsequently diluted 1:2 in sterile PBS; 2,500 HAU of virus in 400 µl was injected per mouse. For i.m. immunizations, 10 µg of purified virus in 25 µl PBS was UV-inactivated on ice for 6 min; the inactivated virus was mixed with 25 µl Titermax Gold adjuvant (Sigma) and injected into the caudal thigh of mice. For $CD4^+$ T cell depletion, the mAb GK1.5 was administered intraperitoneally 1 d before infection or immunization and subsequently every third day. Depletion was confirmed by flow cytometry. H28-E23 Fab was pre-incubated with UV-inactivated PR8 virus for 1 h at 22 °C before i.p. injection.

ELISA and serum quantification. Macrolon medium-binding half-well ELISA plates (Greiner Biotech) were coated overnight at 4 °C with purified HAs in 25 µl PBS. Plates were blocked with 50 µl PBS plus 4% milk for 2 h at 22 °C. After three washes with PBS + 0.05% Tween-20 (PBST), the plates were incubated with 25 µl of sera that was serially diluted twofold starting from 1:100 in PBST for 1 h at 22 °C. After three washes, the plates were incubated with 25 µl of horseradish peroxidase (HRP)-conjugated rat anti-mouse-κ (Southern Biotech) diluted 1:1,000 for 1 h at 22 °C. For heavy-chain determination, plates were incubated with biotinylated anti-mouse-IgG/IgM followed by incubation with avidin-D-peroxidase (VectorLab). After three washes, the plates were developed for 5 min using TMB substrate (KPL Biomedical), after which the reaction was stopped by the addition of 0.1 N HCl. Plates were read at 450 nm. ELISA binding was expressed as area under the curve (AUC), as it better captured changes in both affinity and maximum binding of the pAbs. Curves and AUCs were determined using GraphPad Prism software.

Hemagglutination inhibition (HI) and microneutralization. HI assays were performed in 96-well round-bottom plates as previously described[15]. Briefly, serum was serially diluted and incubated with 4 HAU PR8 for 30 min at 22 °C before adding 1% turkey red blood cells for 1 h at 22 °C. Microneutralization assays on MDCK cells were also performed as described previously[15], with minor modifications—twofold-diluted serum was incubated for 30 min at 37 °C with 100 $TCID_{50}$ of PR8 before its addition to confluent MDCK cells for 1 h at 37 °C. Cells were washed, and the medium was replaced with one containing 1 µg/ml of L-1-tosylamide-2-phenylethyl chloromethyl ketone (TPCK)-treated trypsin. Cytopathic effects were assessed after 4 d.

Flow cytometric detection of rHA-specific germinal center B cells. The procedure was nearly identical to the one described[22], with a few modifications. MLNs or spleens were harvested from euthanized mice at different times after infection or immunization. Single-cell suspensions were stained with the following labeled mAbs: anti-CD3ε–PacificBlue (cat. no. 558214), anti-B220–PE–Cy7 (cat. no. 25-0452-82; eBioscience), anti-CD38–FITC (cat. no. 558813) and anti-GL7–PE (cat. no. 561530) (BD Biosciences, unless otherwise stated). rHA was used at 0.1 µg/ml and detected using streptavidin–APC (cat. no. 17-4317-82; eBioscience). Cell viability was assessed using 10 µg/ml ethidium mono-azide bromide (EMA) (ThermoFisher). Samples were analyzed using a BD LSRFortessa X-20 instrument. Analysis was performed using FlowJo software (TreeStar).

AC_{50} measurement of the affinity of the germinal center B cell population. MLNs were prepared and stained as described above, using a low number of cells per tube (1×10^4 to 2×10^4 antigen-specific cells per tube), and incubated with a graded concentration of rHA (0.66 nM to 66 nM). Data were plotted using the frequency of rHA-positive B cells versus rHA concentration, and 50% maximal binding (AC_{50}) was calculated using a single one-site binding with a Hill slope calculation[22].

Enzyme-linked immunospot (ELISPOT) detection of antibody-secreting cells (ASCs). PVDF plates (EMD Millipore) were activated with 35% ethanol for 5 min at 22 °C. After substantial washing of the plates with distilled water and PBS, the wells were coated overnight at 22 °C in a humid chamber with 0.75 µg of goat anti-mouse-IgG (Jackson Laboratories) in PBS.

At days 3, 7, 9, 14 and 17, MLNs were excised and individually processed to a single-cell suspension. Plates were blocked with PBS plus 2% BSA for 1 h at 22 °C and washed with PBST and RPMI medium (ThermoFisher Scientific). Cells were incubated in serial twofold dilutions, starting at 5×10^5 cells, in RPMI medium plus 7% FCS for 18–20 h at 37 °C.

Cells were lysed with extensive washes with distilled water. Plates were then incubated with 5 ng of rHA per well for 2 h at 22 °C. Detection was carried out after a 1-h incubation with avidin D-HRP (VectorLabs) at 1:1,000 by a 10-min incubation with AEC substrate set (BD Biosciences). Spots were counted for each well with a CTL ImmunoSpot analyzer, and data were analyzed with the CTL ImmunoSpot software.

Lymph node sectioning and germinal center staining. MLNs or spleen segments were fixed in PLP fixative (periodate–lysine–paraformaldehyde) overnight, as reported previously[45], cryoprotected in 15% sucrose, embedded in OCT medium (Electron Microscopy Sciences) and frozen in dry-ice-cooled isopentane. Sixteen-micrometer sections were cut on a Leica cryostat (Leica Microsystems), blocked with 5% goat or donkey serum, stained with a combination of antibodies to B220 (clone RA3-6B2), GL-7 (clone GL-7) and CD38 (clone 90) (all from eBioscience), and detected using fluorescently labeled secondary antibodies (Alexa-Fuor-488- or Alexa-Fluor-568-conjugated goat anti-rat immunoblobulin; cat. no. A-11006 and A-11077, respectively; ThermoFisher Scientific). For controls, sections were incubated with secondary antibodies only. All images were acquired with identical photomultiplier-tube (PMT) and laser settings on a Leica SP5 confocal microscope.

Statistical analysis. AUCs and all curves were calculated using one-site binding with Hill slope curve fitting. Correlation was assessed using the Pearson correlation coefficient. Sample size for animal studies was based on previous experience. Animal studies were performed without blinding. One-way analysis of variance with a *post hoc* Tukey's multiple-comparison

doi:10.1038/ni.3680

test was applied as indicated in the figure legends. All were determined using GraphPad Prism (GraphPad Software Inc.).

Data availability. All of the reagents described in the study and the data that support the findings reported are available from J.W.Y. upon request.

44. Yewdell, J.W. & Gerhard, W. Antigenic characterization of viruses by monoclonal antibodies. *Annu. Rev. Microbiol.* **35**, 185–206 (1981).
45. Pieri, L., Sassoli, C., Romagnoli, P. & Domenici, L. Use of periodate–lysine–paraformaldehyde for the fixation of multiple antigens in human skin biopsies. *Eur. J. Histochem.* **46**, 365–375 (2002).